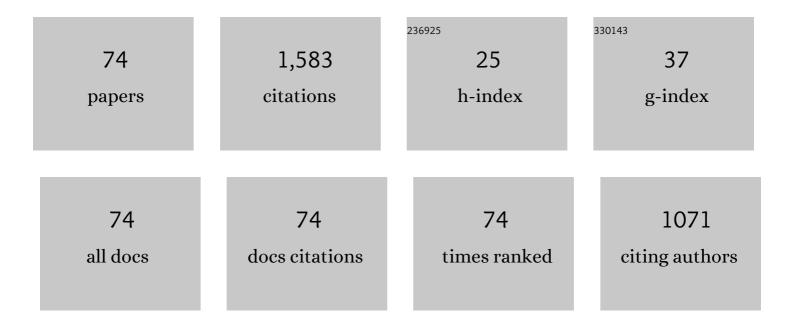
Faramarz Hossein-Babaei

List of Publications by Year in descending order

Source: https://exaly.com/author-pdf/5621750/publications.pdf Version: 2024-02-01



#	Article	IF	CITATIONS
1	Compensation for the drift-like terms caused by environmental fluctuations in the responses of chemoresistive gas sensors. Sensors and Actuators B: Chemical, 2010, 143, 641-648.	7.8	95
2	A breakthrough in gas diagnosis with a temperature-modulated generic metal oxide gas sensor. Sensors and Actuators B: Chemical, 2012, 166-167, 419-425.	7.8	84
3	Recognition of complex odors with a single generic tin oxide gas sensor. Sensors and Actuators B: Chemical, 2014, 194, 156-163.	7.8	73
4	The energy barrier at noble metal/TiO2 junctions. Applied Physics Letters, 2015, 106, .	3.3	73
5	Analysis of thickness dependence of the sensitivity in thin film resistive gas sensors. Sensors and Actuators B: Chemical, 2003, 89, 256-261.	7.8	62
6	A resistive gas sensor based on undoped p-type anatase. Sensors and Actuators B: Chemical, 2005, 110, 28-35.	7.8	60
7	Gas Analysis by Monitoring Molecular Diffusion in a Microfluidic Channel. Analytical Chemistry, 2010, 82, 8349-8355.	6.5	46
8	Forming ohmic Ag/SnO2 contacts. Materials Letters, 2015, 141, 141-144.	2.6	46
9	Separate assessment of chemoresistivity and Schottky-type gas sensitivity in M–metal oxide–M′ structures. Sensors and Actuators B: Chemical, 2011, 160, 174-180.	7.8	45
10	Titanium and silver contacts on thermally oxidized titanium chip: Electrical and gas sensing properties. Solid-State Electronics, 2011, 56, 185-190.	1.4	43
11	A miniature gas analyzer made by integrating a chemoresistor with a microchannel. Lab on A Chip, 2012, 12, 1874.	6.0	43
12	Large area Ag–TiO2 UV radiation sensor fabricated on a thermally oxidized titanium chip. Sensors and Actuators A: Physical, 2012, 173, 116-121.	4.1	43
13	Electrophoretically deposited zinc oxide thick film gas sensor. Electronics Letters, 2000, 36, 1815.	1.0	42
14	Electronic Conduction in Ti/Poly-TiO2/Ti Structures. Scientific Reports, 2016, 6, 29624.	3.3	39
15	Alteration of pore size distribution by sol–gel impregnation for dynamic range and sensitivity adjustment in Kelvin condensation-based humidity sensors. Sensors and Actuators B: Chemical, 2014, 191, 572-578.	7.8	38
16	Assessing the diagnostic information in the response patterns of a temperature-modulated tin oxide gas sensor. Measurement Science and Technology, 2011, 22, 035201.	2.6	35
17	Porous silver-TiO2 Schottky-type chemical sensor fabricated on thermally oxidised titanium. Electronics Letters, 2008, 44, 161.	1.0	34
18	Analyzing the Responses of a Thermally Modulated Gas Sensor Using a Linear System Identification Technique for Gas Diagnosis. IEEE Sensors Journal, 2008, 8, 1837-1847.	4.7	31

#	Article	IF	CITATIONS
19	Extracting discriminative information from the Padé-Z-transformed responses of a temperature-modulated chemoresistive sensor for gas recognition. Sensors and Actuators B: Chemical, 2009, 142, 19-27.	7.8	31
20	Gas Sensitive Porous Silver-Rutile High-Temperature Schottky Diode on Thermally Oxidized Titanium. IEEE Sensors Journal, 2009, 9, 237-243.	4.7	31
21	The selective flow of volatile organic compounds in conductive polymer-coated microchannels. Scientific Reports, 2017, 7, 42299.	3.3	31
22	Gas diagnosis by a quantitative assessment of the transient response of a capillary-attached gas sensor. Sensors and Actuators B: Chemical, 2005, 107, 461-467.	7.8	30
23	Ten micron-thick undoped SnO2 layers grown by spray pyrolysis for microheater fabrication. Materials Letters, 2017, 196, 104-107.	2.6	30
24	A Novel Approach to Hydrogen Sensing. IEEE Sensors Journal, 2004, 4, 802-806.	4.7	29
25	Gas diagnosis based on selective diffusion retardation in an air filled capillary. Sensors and Actuators B: Chemical, 2003, 96, 298-303.	7.8	27
26	Linking thermoelectric generation in polycrystalline semiconductors to grain boundary effects sets a platform for novel Seebeck effect-based sensors. Journal of Materials Chemistry A, 2018, 6, 10370-10378.	10.3	27
27	Electrophoretic deposition of MgO thick films from an acetone suspension. Journal of the European Ceramic Society, 2000, 20, 2165-2168.	5.7	26
28	Growth of ZnO nanorods on the surface and edges of a multilayer graphene sheet. Scripta Materialia, 2017, 139, 77-82.	5.2	25
29	Zinc oxide-based direct thermoelectric gas sensor for the detection of volatile organic compounds in air. Sensors and Actuators B: Chemical, 2019, 294, 245-252.	7.8	25
30	Diffusion Bonding of Metal Wires Directly to the Functional Metal Oxide Semiconductors for Forming Reliable Electrical Contacts. ACS Applied Materials & Interfaces, 2017, 9, 26637-26641.	8.0	24
31	Dopant passivation by adsorbed water monomers causes high humidity sensitivity in PEDOT: PSS thin films at ppm-level humidity. Sensors and Actuators B: Chemical, 2019, 293, 329-335.	7.8	24
32	Transient regime of gas diffusion-physisorption through a microporous barrier. IEEE Sensors Journal, 2005, 5, 1004-1010.	4.7	23
33	Electronic properties of Ag-doped ZnO: DFT hybrid functional study. Physical Chemistry Chemical Physics, 2018, 20, 14688-14693.	2.8	22
34	Tin oxide gas sensor on tin oxide microheater for high-temperature methane sensing. Materials Letters, 2020, 263, 127196.	2.6	20
35	A gold/organic semiconductor diode for ppm-level humidity sensing. Sensors and Actuators B: Chemical, 2014, 205, 143-150.	7.8	19
36	The ohmic contact between zinc oxide and highly oriented pyrolytic graphite. Materials Letters, 2017, 192, 52-55.	2.6	17

#	Article	IF	CITATIONS
37	Identifying volatile organic compounds by determining their diffusion and surface adsorption parameters in microfluidic channels. Sensors and Actuators B: Chemical, 2015, 220, 607-613.	7.8	15
38	A concept of microfluidic electronic tongue. Microfluidics and Nanofluidics, 2012, 13, 331-344.	2.2	14
39	Transient molecular diffusion in microfluidic channels: Modeling and experimental verification of the results. Sensors and Actuators B: Chemical, 2016, 233, 646-653.	7.8	14
40	Electrophoretic deposition of ZnO on highly oriented pyrolytic graphite substrates. Materials Letters, 2017, 209, 404-407.	2.6	14
41	Diffusion-physisorption of a trace material in a capillary tube. Journal of Applied Physics, 2006, 100, 124917.	2.5	12
42	Apparatus for Seebeck Coefficient Measurements on High-Resistance Bulk and Thin-film Samples. IEEE Transactions on Instrumentation and Measurement, 2020, 69, 3070-3077.	4.7	12
43	Air-stable electrical conduction in oxidized poly[2-methoxy-5-(2-ethylhexyloxy)-p-phenylene vinylene] thin films. Applied Physics Letters, 2013, 103, .	3.3	11
44	Seebeck voltage measurement in undoped metal oxide semiconductors. Measurement Science and Technology, 2017, 28, 115002.	2.6	11
45	Growing continuous zinc oxide layers with reproducible nanostructures on the seeded alumina substrates using spray pyrolysis. Ceramics International, 2020, 46, 8567-8574.	4.8	11
46	Atmospheric Dependence of Thermoelectric Generation in SnO ₂ Thin Films with Different Intergranular Potential Barriers Utilized for Self-Powered H ₂ S Sensor Fabrication. ACS Applied Electronic Materials, 2021, 3, 353-361.	4.3	11
47	Oxygen adsorption at noble metal/TiO ₂ junctions. IOP Conference Series: Materials Science and Engineering, 2016, 108, 012030.	0.6	9
48	A microfluidic gas analyzer for selective detection of biomarker gases. , 2012, , .		7
49	Hydrogen Detection with Noble Metal-TiO2 Schottky Diodes. Key Engineering Materials, 0, 495, 289-293.	0.4	6
50	Quantitative Assessment of Vapor Molecule Adsorption to Solid Surfaces by Flow Rate Monitoring in Microfluidic Channels. Analytical Chemistry, 2019, 91, 12827-12834.	6.5	6
51	Direct current powered humidity sensor based on a polymer composite with humidity sensitive electronic conduction. Applied Physics Letters, 2020, 117, .	3.3	5
52	Electrical Resistance and Seebeck Effect in Undoped Polycrystalline Zinc Oxide. Key Engineering Materials, 0, 605, 185-188.	0.4	4
53	Pressure Sensitivity of Charge Conduction Through the Interface Between a Metal Oxide Nanocrystallite and Graphene. Advanced Materials Interfaces, 2021, 8, 2001815.	3.7	4
54	Fabrication of poly-Si thick films by electrophoretic deposition. Electronics Letters, 2001, 37, 1090.	1.0	3

#	Article	IF	CITATIONS
55	Wide dynamic range hydrogen sensing using silver-rutile Schottky diode. , 2008, , .		3
56	Ti/PEDOT:PSS/Ti Pressure Sensor., 2019,,.		3
57	Obtaining Highly Selective Responses from a Bulk Tin Oxide Gas Sensor. Key Engineering Materials, 0, 543, 239-242.	0.4	2
58	Differentiating among Gas Mixtures Using a Single Tin Oxide Gas Sensor. Key Engineering Materials, 0, 605, 189-193.	0.4	2
59	A model for the electric conduction in metal/poly-TiO ₂ /metal structure. Journal of Physics: Conference Series, 2017, 939, 012010.	0.4	2
60	Hydrogen Level Detection via Thermal Conductivity Measurement Using Temporal Temperature Monitoring. , 2019, , .		2
61	P2MM.8 - Conduction Activation Energy in PEDOT:PSS Thin Films. , 2018, , .		2
62	Online Gas Diagnosis by a Capillary-attached Gas Sensor Coupled to a Pattern Recognition System. , 2006, , .		1
63	Porosity modification for the adjustment of the dynamic range of ceramic humidity sensors. , 2008, , .		1
64	Single Sensor Gas Analysis Using a Microfluidic Channel. Key Engineering Materials, 0, 495, 302-305.	0.4	1
65	A Graphene Oxide-Based Humidity Sensor for Wearable Electronic. , 2019, , .		1
66	Si/SiO2/Ag optical sensor. , 2021, , .		1
67	Gas Diagnosis by the application of system identification technique on the response of a thermally modulated semiconductor gas sensor. , 2006, , .		0
68	Silver-Rutile UV Sensor Fabricated on Thermally Oxidized Titanium Foil . Key Engineering Materials, 2011, 495, 18-22.	0.4	0
69	Discriminating among Acid-, Base-, and Salt-Based Electrolytes Using a Single Microfluidic Channel. Key Engineering Materials, 0, 543, 285-288.	0.4	0
70	A Novel Material for Chemical Sensor Applications: Oxidized MEH-PPV. Key Engineering Materials, 0, 644, 12-15.	0.4	0
71	Bipolar Resistive Switching of an Al/ZnO/Ti-based Memristor. , 2019, , .		0
72	SnO2:F Films Grown by Ultrasonic Spray Pyrolysis Suitable for Transparent Defogger Fabrication. , 2019, , .		0

#	Article	IF	CITATIONS
73	Classification of Dairy Products using Chronoamperometry Performed in a Microfluidic Channel. , 2019, , .		0
74	Space-charge-limited current through the electrophoretically formed TiO2/HOPG junction. , 2020, , .		0